Higgs total width at the ATLAS experiment

Rafael Coelho Lopes de Sá
on behalf of the ATLAS Collaboration

UMassAmherst

CERN Seminar

Nov 15th, 2022

The Higgs boson

The Higgs Boson was discovered in 2012 by ATLAS and CMS

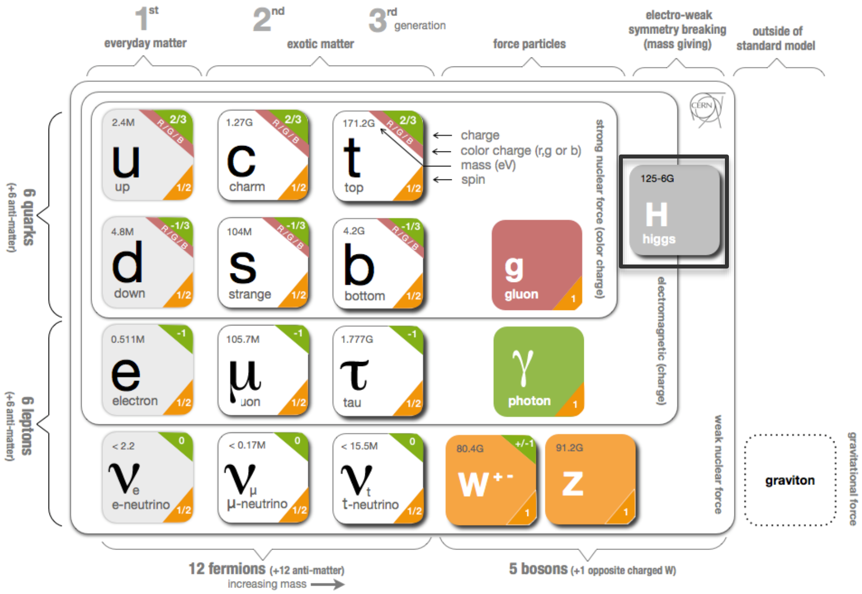

Characterization of the Higgs boson properties

Mass
Width
Spin/Parity
Couplings

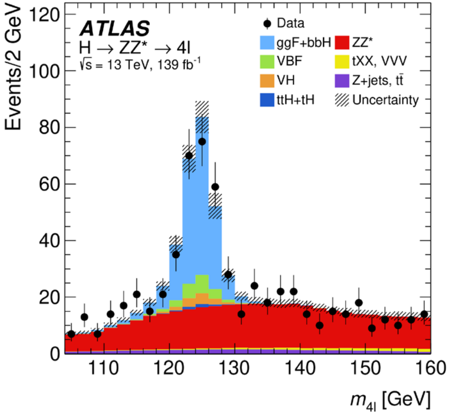

This talk will focus on results using the $H \rightarrow ZZ$ decay channel

The Higgs boson spin-parity

UMassAmherst ATLAS EXPERIMENT

Spin-parity nature of the Higgs boson has been well established with Run 1 measurements

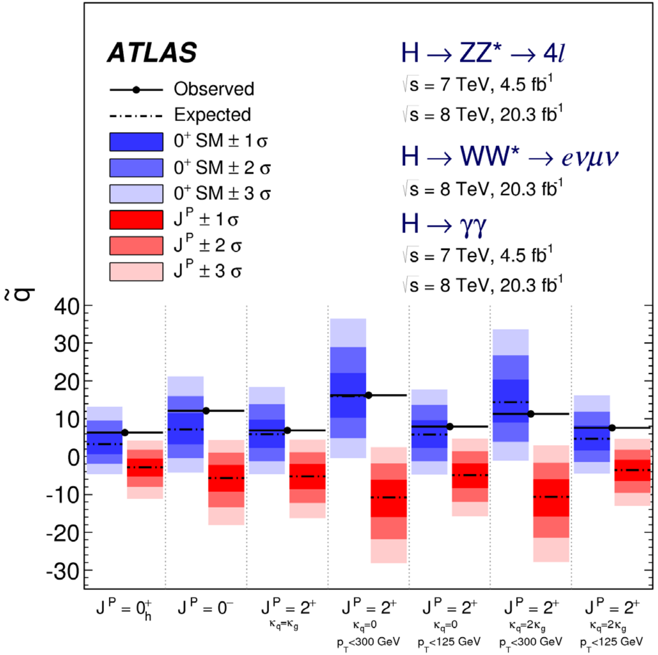

The $J^P = 0^+$ nature of the Higgs boson is greatly favored over other hypothesis with spin 2 or negative parity.

Spin 1 hypothesis excluded by the Landau-Yang theorem.

This result will be explored in the measurement presented today.

ATLAS Collaboration, Eur. Phys. J. C 75 (2015) 476

The Higgs mass

Increasingly precise measurement of the Higgs mass with Run 2 data

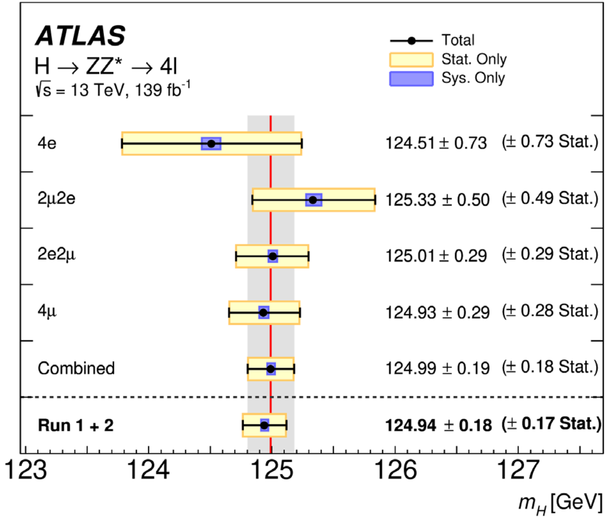

$$m_H = 124.99 \pm 0.18(\text{stat}) \pm 0.04(\text{syst})\ \text{GeV}$$

ATLAS Collaboration, Submitted to PLB, arXiv:2207.00320

Systematic Uncertainty	Contribution [MeV]
Muon momentum scale	±28
Electron energy scale	±19
Signal-process theory	±14

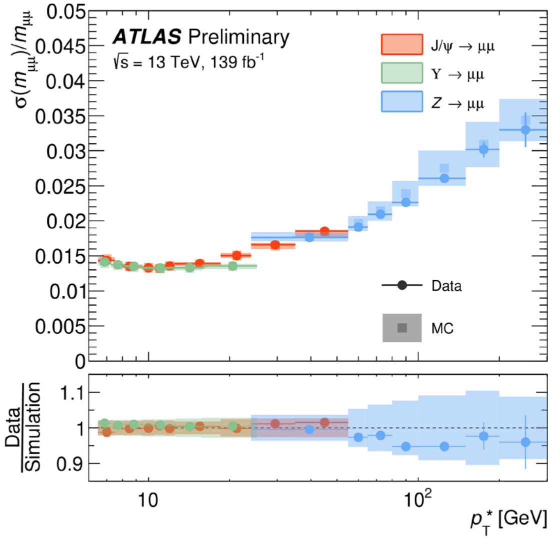

ATLAS Collaboration, MUON-2022-01

Measurement with very small systematic uncertainty.
Excellent work from the object working groups.

The Higgs width

The decay widths of the Higgs boson in the Standard Model are small compared to its mass

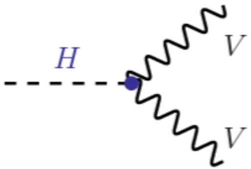

decay to off-shell weak bosons
$H \to VV^*$

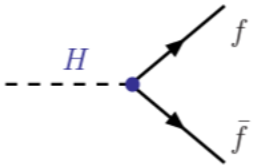

small Yukawa coupling
$H \to ff$ (not the top quark)

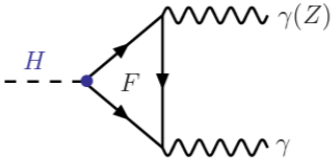

loop-suppressed
$H \to \gamma\gamma$ and $H \to Z\gamma$

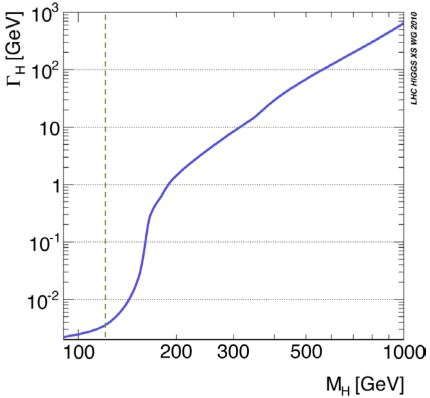

The best estimate of the Higgs boson total width is:

$$\Gamma_H^{SM} = 4.07 \text{ MeV}$$

3 orders of magnitude smaller than our mass resolution

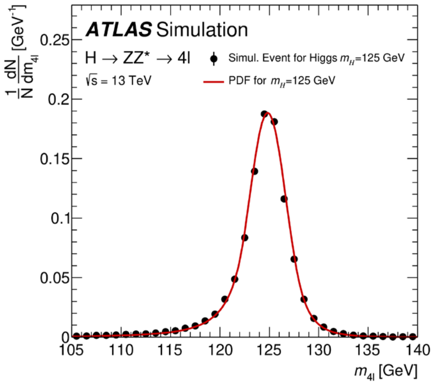

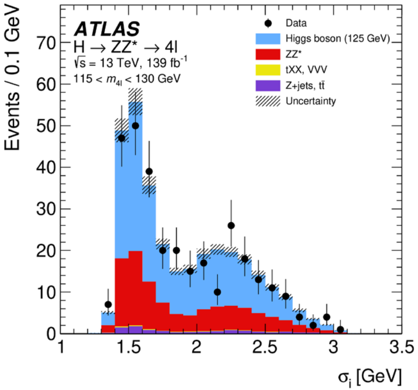

Direct measurements of the width using the Higgs line shape [1]:

$$\Gamma_H < 2.6 \text{ GeV @ 95\% CL.}$$

Measurements of the lifetime [2]:

$$\Gamma_H > 3.5 \times 10^{-9} \text{ MeV @ 95\% CL.}$$

[1] Phys. Rev. D 90, 052004 (2014)
[2] Phys. Rev. D92, 072010

On-shell interference and Γ_H

In 2013, L. Dixon and Y. Li [3] pointed out there is a large interference between $H \to \gamma\gamma$ and the continuous $\gamma\gamma$ that can be used to probe the Higgs boson width Γ_H

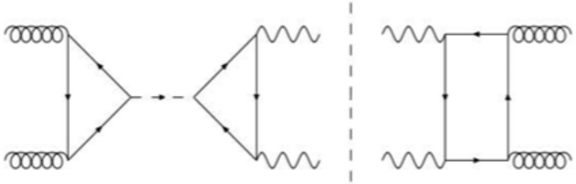

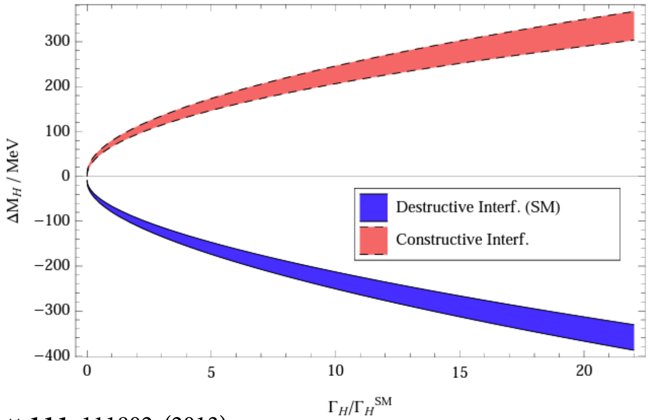

The interference creates a shift in the $m_{\gamma\gamma}$ peak with respect to m_H.

The shift can be used probe Γ_H experimentally by comparing the $m_{\gamma\gamma}$ and $m_{4\ell}$ peaks.

A short note describing an experimental implementation of the method was made public in 2016: ATLAS Collaboration, ATL-PHYS-PUB-2016-009

This method should be able to constrain

$$\Gamma_H/\Gamma_H^{SM} < O(100)$$

[3] Phys Rev Lett **111**, 111802 (2013)

Off-shell Higgs production and Γ_H

UMassAmherst ATLAS EXPERIMENT

In 2012, N. Kauer and G. Passarino [4] pointed out that, despite the small total width, the off-shell Higgs production cross section in $H \to VV$ is not small due threshold enhancements

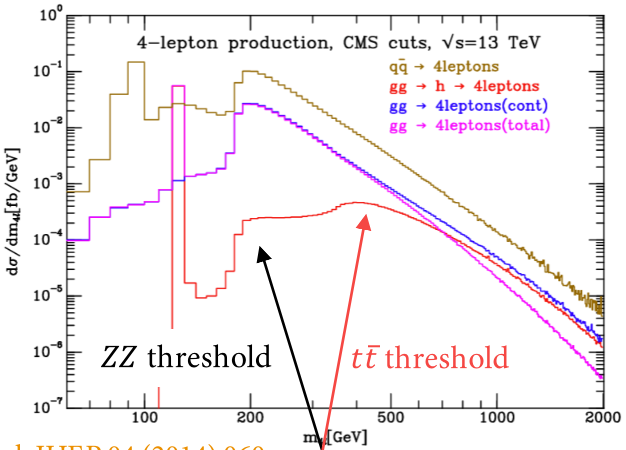

J. Campbell et al. JHEP 04 (2014) 060

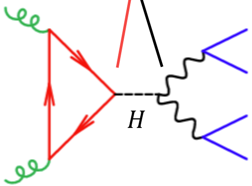

In 2013, F. Caola & K. Melnikov [5] and J. Campbell, R. Keith Ellis & C. Williams [6] argued that this observation could be used to probe Γ_H

$$\frac{d\sigma^{pp\to H\to ZZ}}{dm_{ZZ}} \propto \frac{g_{Hgg}^2 g_{HZZ}^2}{(m_{ZZ}^2 - m_H^2)^2 + m_H^2\Gamma_H^2}$$

on-shell

$$\sigma_{\text{on-shell}}^{pp\to H\to ZZ} \propto \frac{g_{Hgg}^2 g_{HZZ}^2}{m_H \Gamma_H}$$

off-shell

$$\frac{d\sigma_{\text{off-shell}}^{pp\to H\to ZZ}}{dm_{ZZ}} \propto \frac{g_{Hgg}^2 g_{HZZ}^2}{(m_{ZZ}^2 - m_H^2)^2}$$

[4] JHEP 08 (2012) 116
[5] Phys. Rev. D88 (2013) 054024
[6] JHEP 04 (2014) 60

Off-shell Higgs production and Γ_H

UMassAmherst ATLAS EXPERIMENT

In 2012, N. Kauer and G. Passarino [4] pointed out that, despite the small total width, the off-shell Higgs production cross section in $H \to VV$ is not small due threshold enhancements

D. Gonçalves et al. Phys. Rev. D 98, 015023 (2018)

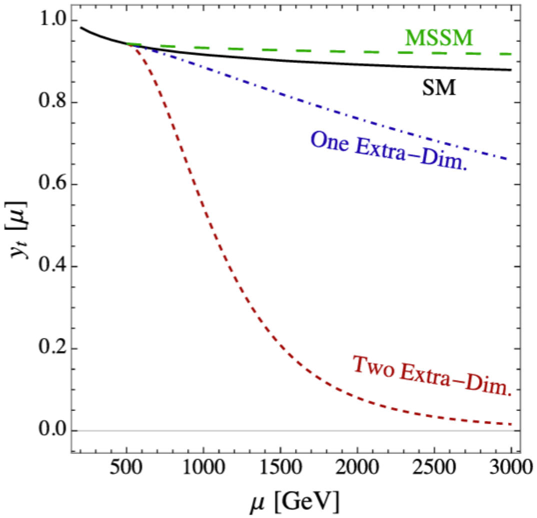

In 2013, F. Caola & K. Melnikov [5] and J. Campbell, R. Keith Ellis & C. Williams [6] argued that this observation could be used to probe Γ_H

The method assumes that that coupling constants evolve like in SM

$$R_{gg} = \frac{\kappa^2_{g,\text{off-shell}}}{\kappa^2_{g,\text{on-shell}}} = 1$$

$$R_{VV} = \frac{\kappa^2_{V,\text{off-shell}}}{\kappa^2_{V,\text{on-shell}}} = 1$$

$$\mu_{\text{on-shell}} = \frac{\sigma^{pp\to H\to ZZ}_{\text{on-shell}}}{\sigma^{pp\to H\to ZZ}_{\text{on-shell,SM}}} = \frac{\kappa^2_{g,\text{on-shell}}\kappa^2_{V,\text{on-shell}}}{\Gamma_H/\Gamma_H^{\text{SM}}}$$

$$\mu_{\text{off-shell}} = \frac{\sigma^{pp\to H\to ZZ}_{\text{off-shell}}}{\sigma^{pp\to H\to ZZ}_{\text{off-shell,SM}}} = \kappa^2_{g,\text{off-shell}}\kappa^2_{V,\text{off-shell}}$$

ATLAS previous results

Run 2 (36 fb^{-1} $2\ell 2\nu$, 36 fb^{-1} 4ℓ):

$\Gamma_H/\Gamma_H^{\text{SM}} \leq 3.5$ @ 95% CL.

Phys. Lett. B 786 (2018) 223

CMS previous results

Run 2 (138 fb^{-1} $2\ell 2\nu$, 78 fb^{-1} 4ℓ):

$\Gamma_H = 3.2^{+5.3}_{-2.7}$ @ 95% CL.

Nat. Phys. 18 (2022) 1329

[4] JHEP 08 (2012) 116
[5] Phys. Rev. D88 (2013) 054024
[6] JHEP 04 (2014) 60

Signal-background interference

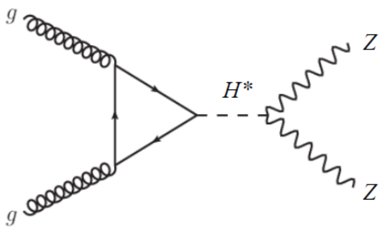

signal (S)
$gg \to H^* \to ZZ$

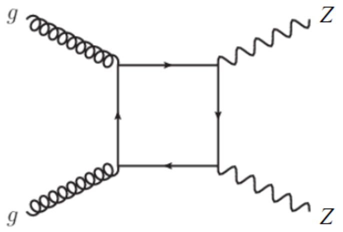

background (B)
$gg \to ZZ$

In the off-shell region, the interference (I) between the two components S and B is large and destructive (to preserve unitarity at high energies).

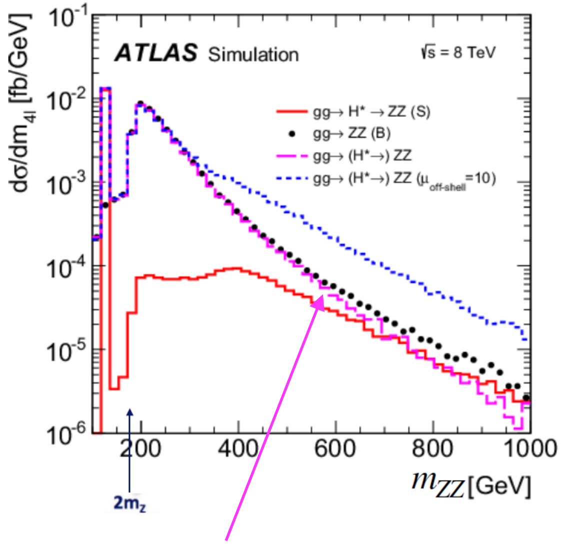

SBI = S + B + I

ggF off-shell Higgs production

The Γ_H result presented today uses the measurement of the off-shell Higgs production with both $H \to ZZ \to 4\ell$ and $H \to ZZ \to 2\ell 2\nu$ decay channels

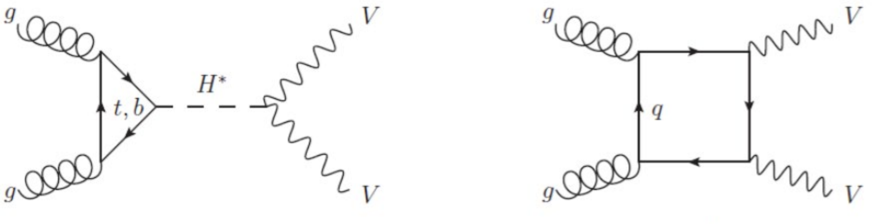

(a) (b)

$$\mu_{\text{off-shell}} = \kappa^2_{g,\text{off-shell}} \kappa^2_{V,\text{off-shell}}$$

$$\mathrm{N}_{gg\to(H^*)\to ZZ}(\mu_{\text{off-shell}}) = \mu_{\text{off-shell}}\,\mathrm{N}_S + \sqrt{\mu_{\text{off-shell}}}\,\mathrm{N}_I + \mathrm{N}_B \qquad \mathrm{N}_I = \mathrm{N}_{SBI} - \mathrm{N}_S - \mathrm{N}_B$$

$$\mathrm{N}_{gg\to(H^*)\to ZZ}(\mu_{\text{off-shell}}) = (\mu_{\text{off-shell}} - \sqrt{\mu_{\text{off-shell}}})\mathrm{N}_S + \sqrt{\mu_{\text{off-shell}}}\,\mathrm{N}_{SBI} + (1 - \sqrt{\mu_{\text{off-shell}}})\mathrm{N}_B$$

The description is done as a function of S, SBI, and B because of the inefficiencies in generating interference-only MC samples. Modern developments motivated by VBF-type production have greatly improved the situation [7].

[7] Eur. Phys. J. C 81 (2021) 5, 435

EW off-shell Higgs production

UMassAmherst ATLAS EXPERIMENT

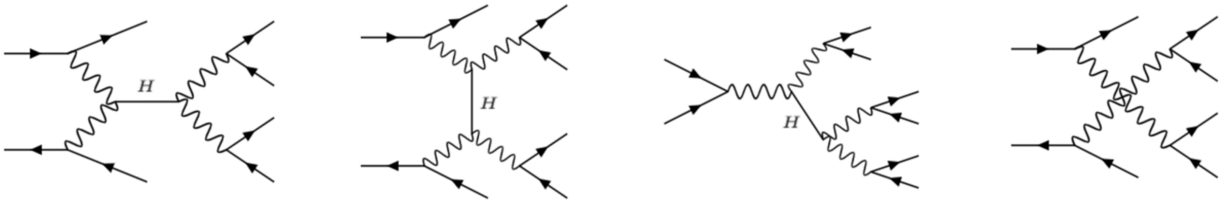

Non-negligible interference between all the components (VBF, t-channel, VH, VBS)

$$\mu_{\text{off-shell}} = \kappa^4_{V,\text{off-shell}}$$

EW samples are always produced as full process (SBI^{EW}), including regions with $m_{4\ell} \simeq 125$ GeV (t-channel Higgs process renders separation impossible).

$$\text{N}_{\text{EW}}(\mu_{\text{off-shell}}) = \begin{bmatrix} \mu_{\text{off-shell}} \\ \sqrt{\mu_{\text{off-shell}}} \\ 1 \end{bmatrix}^{\text{T}} \begin{bmatrix} 0 & 0 & 1 \\ 1 & 1 & 1 \\ 10 & \sqrt{10} & 1 \end{bmatrix}^{-1} \begin{bmatrix} SBI_0^{\text{EW}} \\ SBI_1^{\text{EW}} \\ SBI_{10}^{\text{EW}} \end{bmatrix}$$

Three different values of $\mu_{\text{off-shell}}$ are used (0,1,10)

Off-shell Higgs and global fits

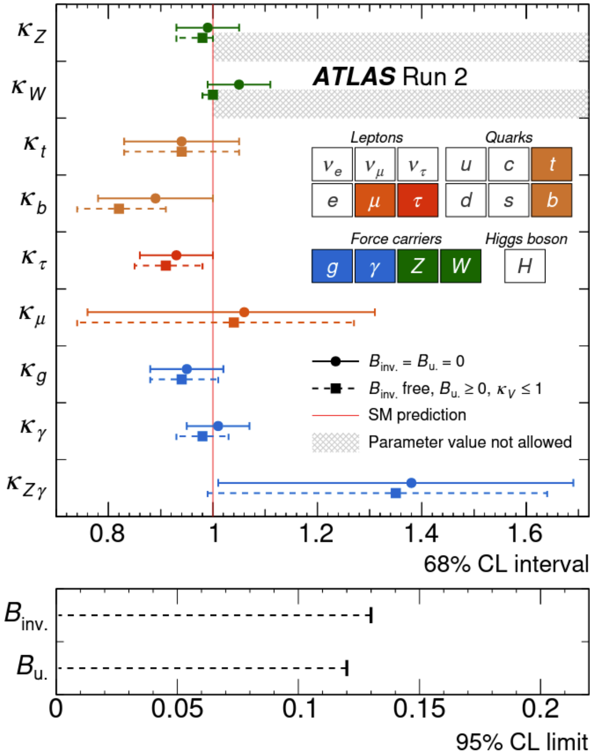

$$\Gamma_H = \Gamma_H^{SM} \frac{\sum_j B_j^{SM} \kappa_j^2}{(1 - B_i - B_u)}$$

B_u (undetected decays of the Higgs boson) scales all observed cross section and we only measure ratios in the LHC.

Constraint on B_u are obtained by requiring $\kappa_V \leq 1$.

Including off-shell Higgs measurement, limits can be obtained without these hypotheses since off-shell production does not depend on Γ_H

ATLAS Collaboration, Nature 607, pages 52-59 (2022)

Off-shell Higgs and global fits

UMassAmherst ATLAS EXPERIMENT

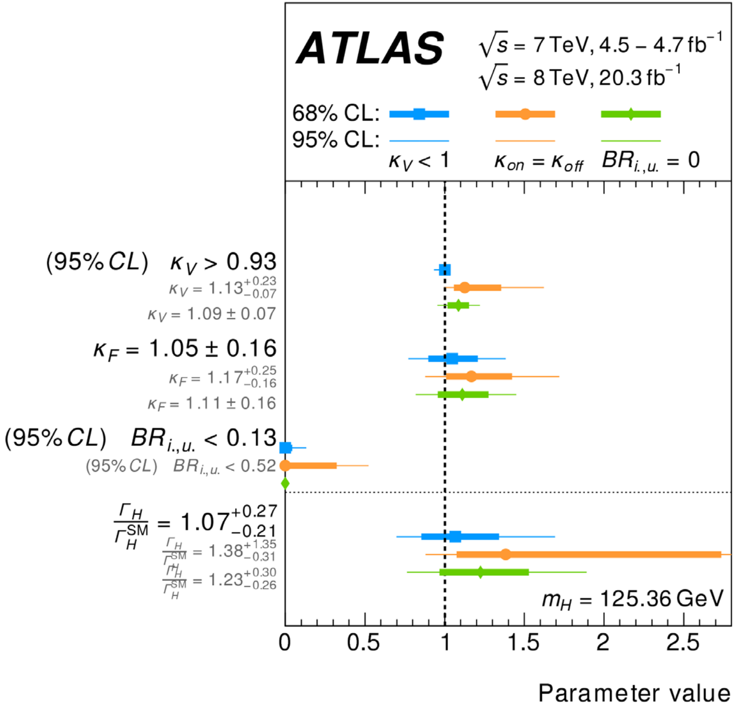

ATLAS Collaboration, Eur. Phys. J. C (2016) 76

$$\Gamma_H = \Gamma_H^{SM} \frac{\sum_j B_j^{SM} \kappa_j^2}{(1 - B_i - B_u)}$$

B_u (undetected decays of the Higgs boson) scales all observed cross section and we only measure ratios in the LHC.

Constraint on B_u are obtained by requiring $\kappa_V \leq 1$.

Including off-shell Higgs measurement, limits can be obtained without these hypotheses since off-shell production does not depend on Γ_H

The two hypotheses were used in the global fits performed with Run 1 data.

Off-shell Higgs and EFT

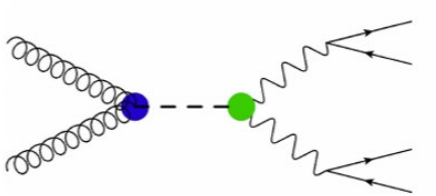

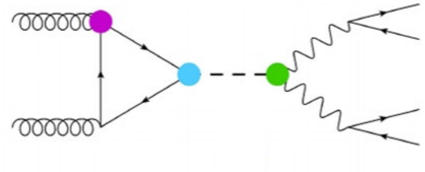

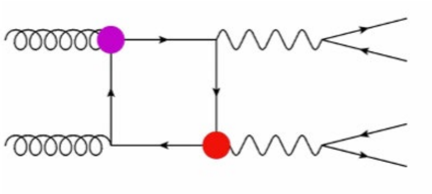

Off-shell Higgs production can be used to probe EFT operators, in both signal and background diagrams.

- Processes probing higher energy scale $m_{ZZ} > m_H$.
- But low number of events because of reduced cross section.

As noted by A. Azatov, C. Grojean, A. Paul, and E. Salvioni [8] in 2015, off-shell production can break the degeneracy between operators that are indistinguishable with on-shell production

This degeneracy can also be broken by $t\bar{t}H$ and boosted Higgs production, as noted by the same authors in [9].

[8] JETP Vol. 147 (3) (2015)
[9] JHEP 1609 (2016) 123

Off-shell Higgs and new light states

- The Higgs width interpretation relies on the assumption that the relationship between the Higgs on-shell and off-shell couplings is given by the SM evolution.
- New BSM light states could break this hypothesis.
- However, new light states would also create new mass thresholds that can be probed with off-shell production.
- In 2018, D. Gonçalves, T. Han, and S. Mukhopadhyay [10] pointed out that off-shell Higgs production can be used to probe light, weakly-coupled BSM particles through new mass thresholds. Interesting searches for HL-LHC.

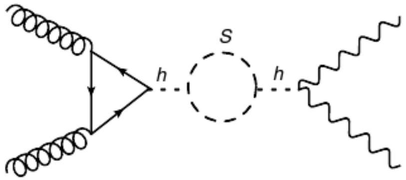

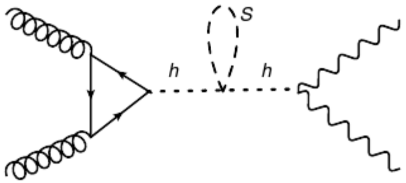

[10] Phys. Rev. D 98, 015023 (2018)

Run 2 ATLAS detector

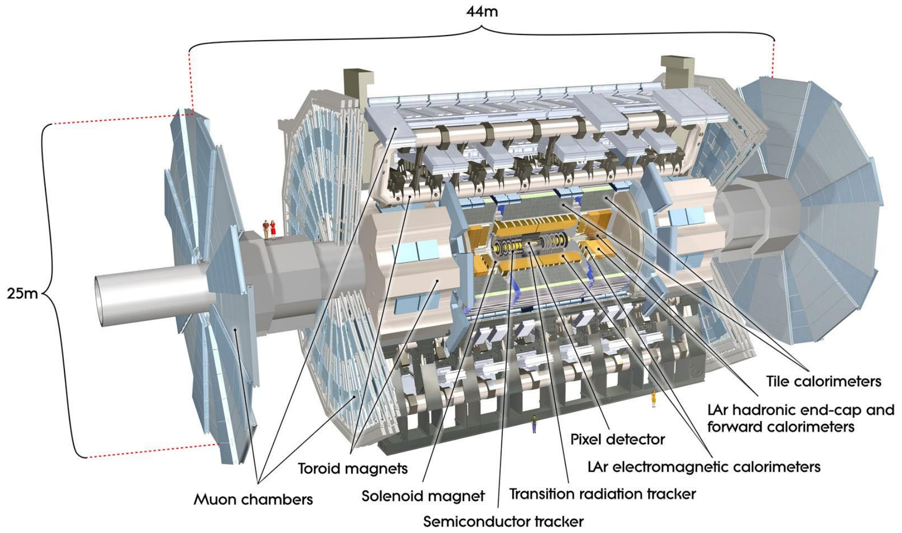

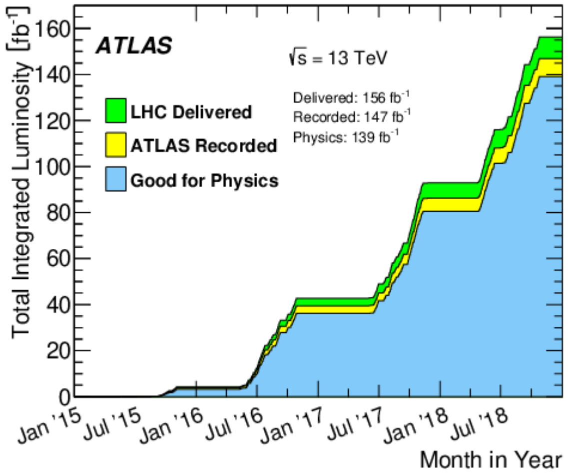

The results presented today use the full Run 2 dataset (139 fb^{-1}) in both $ZZ \to 4\ell$ and $ZZ \to 2\ell 2\nu$ decay channels. They supersede the previous 36 fb^{-1} result.

4ℓ channel → single, double, and triple lepton trigger
$2\ell 2\nu$ channel → single lepton trigger

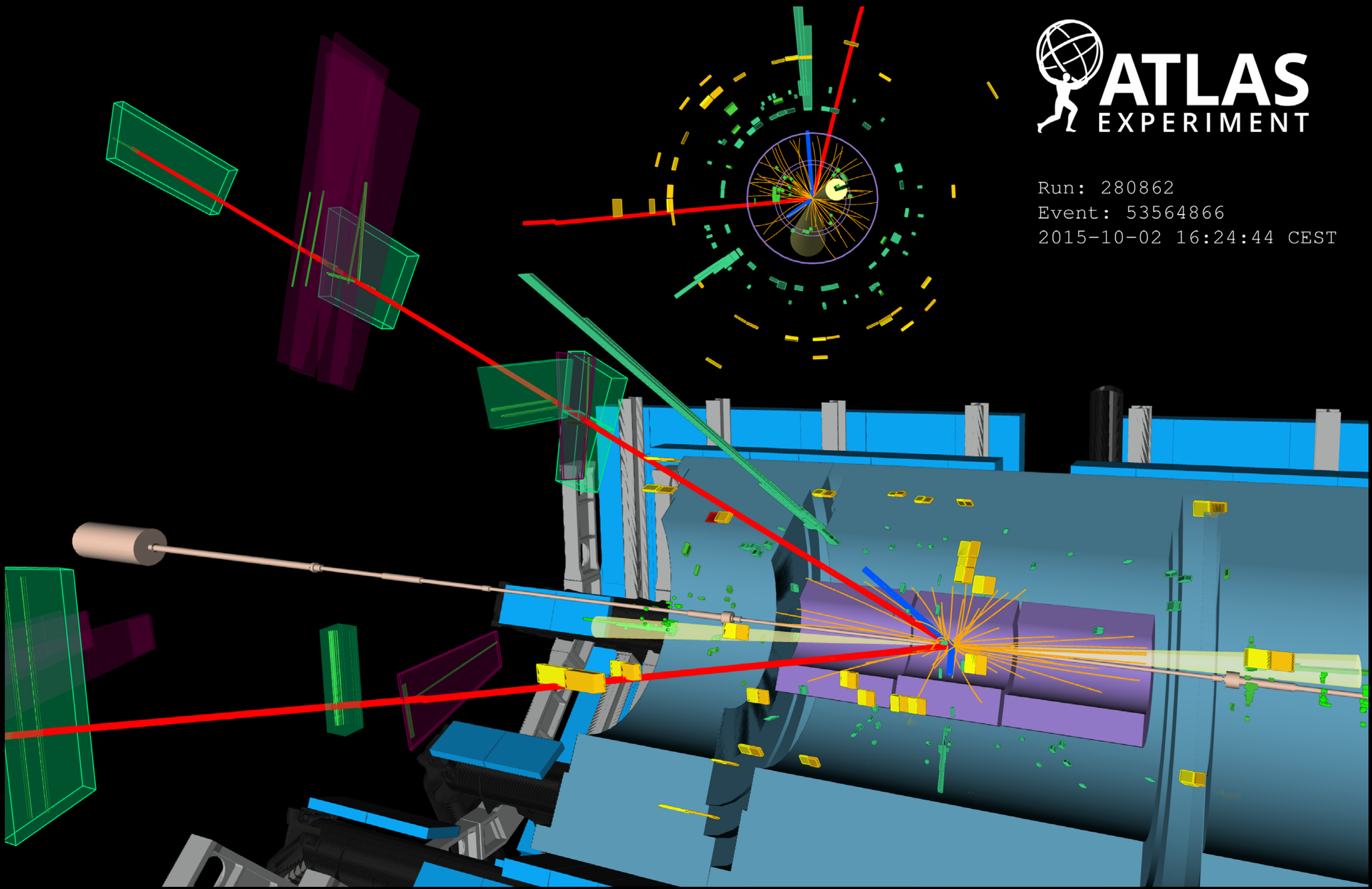
ATLAS
EXPERIMENT
Run: 280862
Event: 53564866
2015-10-02 16:24:44 CEST

Event selection

UMassAmherst ATLAS EXPERIMENT

4ℓ channel

$ZZ \to 4\ell$ selection

2 same-flavor, opposite-charge lepton pairs

Leading $p_T^{\text{lep}} > 20, 15, 10$ GeV

$220 \leq m_{4\ell} \leq 2000$ GeV

$180 \leq m_{4\ell} \leq 220$ GeV (for CRs)

Pair 12 defined as the pair with $m_{\ell\ell}$ closest to m_Z

$50 \leq m_{12} \leq 106$ GeV

$50 - \max(0, \frac{190 - m_{4\ell}}{2}) \leq m_{34} \leq 115$ GeV

$2\ell 2\nu$ channel

$ZZ \to 2\ell 2\nu$ selection

1 same-flavor, opposite-charge lepton pair

Leading $p_T^{\text{lep}} > 30, 20$ GeV

$76 < m_{\ell\ell} < 106$ GeV

$E_T^{\text{miss}} > 120$ GeV

background rejection cuts

3rd lepton veto

$\Delta R_{\ell\ell} < 1.8$

$\Delta\phi(Z, E_T^{\text{miss}}) > 2.5$

$\Delta\phi(\text{jet } p_T > 100 \text{ GeV}, E_T^{\text{miss}}) > 0.4$

E_T^{miss} significance > 10

b-jet veto

Inclusive distributions

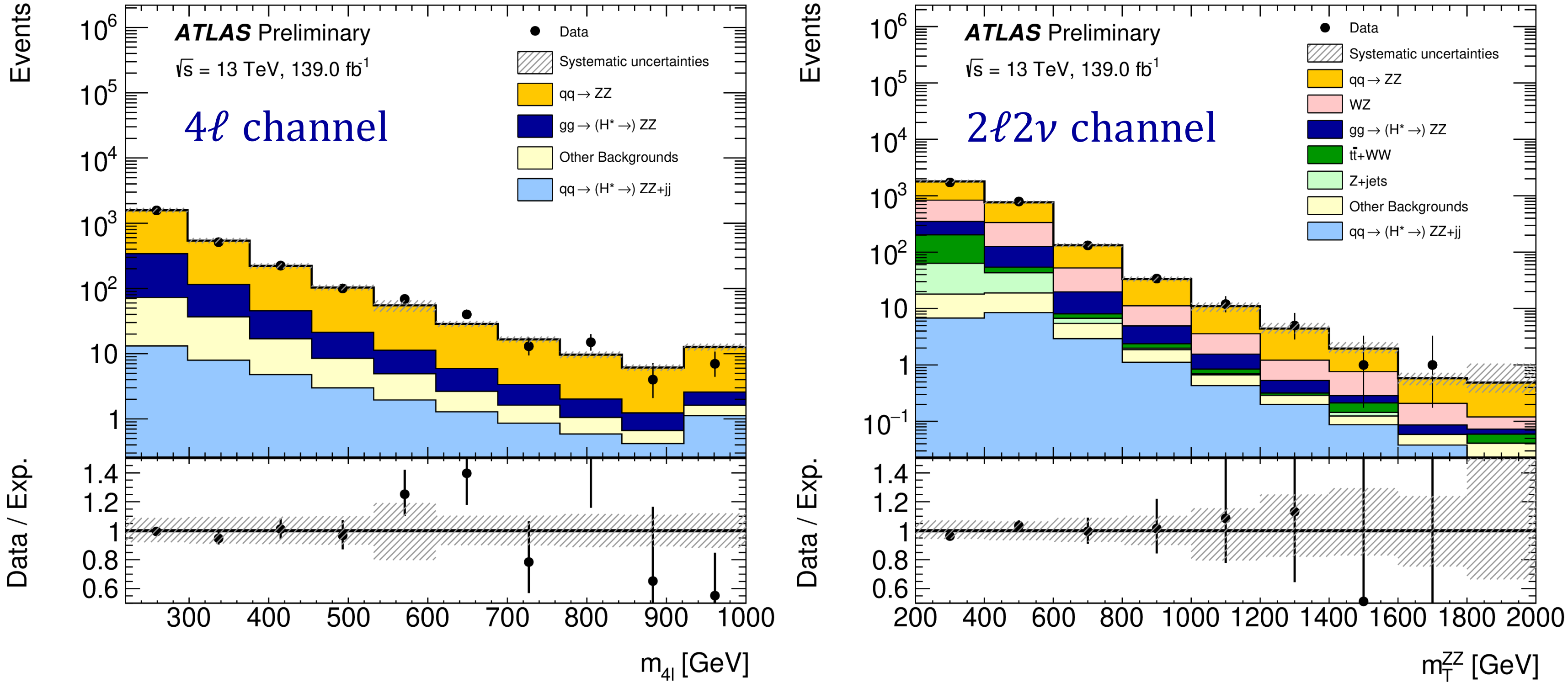

Event categorization

Jets are selected with $p_T > 30$ GeV and $|\eta| < 4.5$

ggF Signal region

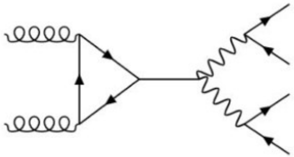

$n_{\text{jets}} = 0$

$n_{\text{jets}} = 1$ and $\eta_j < 2.2$

$n_{\text{jets}} \geq 2$ and $|\Delta\eta_{jj}| < 4.0$

1 jet mixed signal region

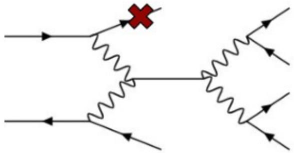

$n_{\text{jets}} = 1$ and $|\eta_j| \geq 2.2$

EW signal region

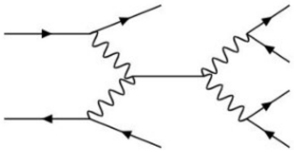

$n_{\text{jets}} \geq 2$ and $|\Delta\eta_{jj}| \geq 4.0$

Fractions in 4ℓ channel

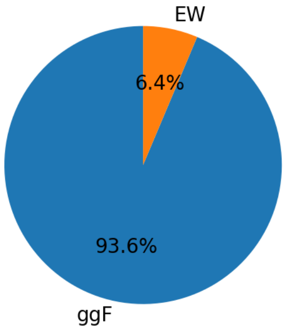

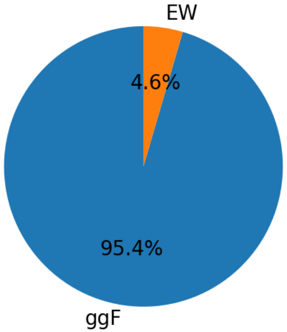

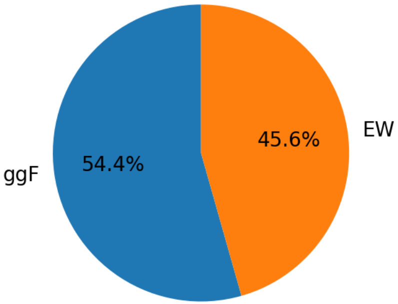

Event categorization

Jets are selected with $p_T > 30$ GeV and $|\eta| < 4.5$

ggF Signal region

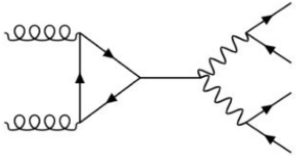

$n_{\text{jets}} = 0$

$n_{\text{jets}} = 1$ and $\eta_j < 2.2$

$n_{\text{jets}} \geq 2$ and $|\Delta\eta_{jj}| < 4.0$

1 jet mixed signal region

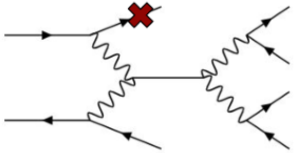

$n_{\text{jets}} = 1$ and $|\eta_j| \geq 2.2$

EW signal region

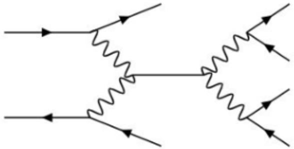

$n_{\text{jets}} \geq 2$ and $|\Delta\eta_{jj}| \geq 4.0$

Fractions in $2\ell 2\nu$ channel

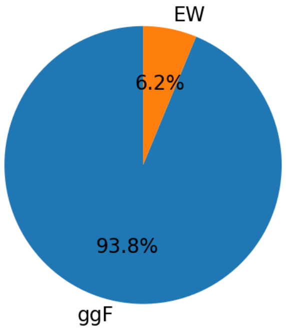

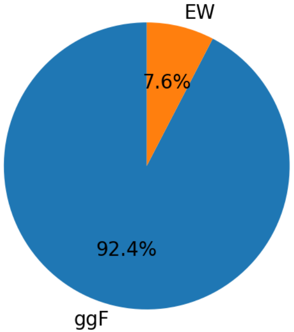

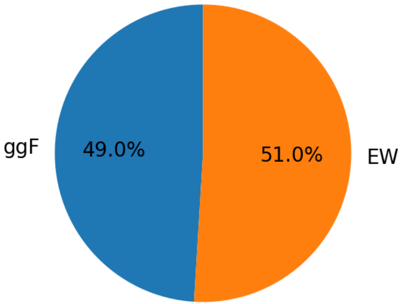

Observable in the 4ℓ channel

- Previous versions of this analysis used analytical matrix element discriminants calculated **without transfer functions**, **without PDFs**, and **with a rough approximation of the initial-state kinematics**.
- This analysis uses a neural network version of the discriminant trained with reconstructed variables and the best higher-order MC simulations available for each process.

ggF region

4ℓ final state full kinematics → dense NN → $O_{\text{NN}}^{\text{ggF}} = \log \frac{P_S^{\text{ggF}}}{P_B^{\text{ggF}} + P_{q\bar{q}ZZ}}$

EW region

$4\ell + 2j$ final state full kinematics → dense NN → $O_{\text{NN}}^{\text{EW}} = \log \frac{P_S^{\text{EW}}}{P_B^{\text{EW}} + P_{q\bar{q}ZZ}}$

NN largely explores the $J_P = 0^+$ nature of the Higgs boson

$O_{\text{NN}}^{\text{ggF}}$ also used for mixed region

Interference cannot be directly included as a category in the NN since it has no probabilistic interpretation (negative weights, not a probability).

Observable in the 4ℓ channel

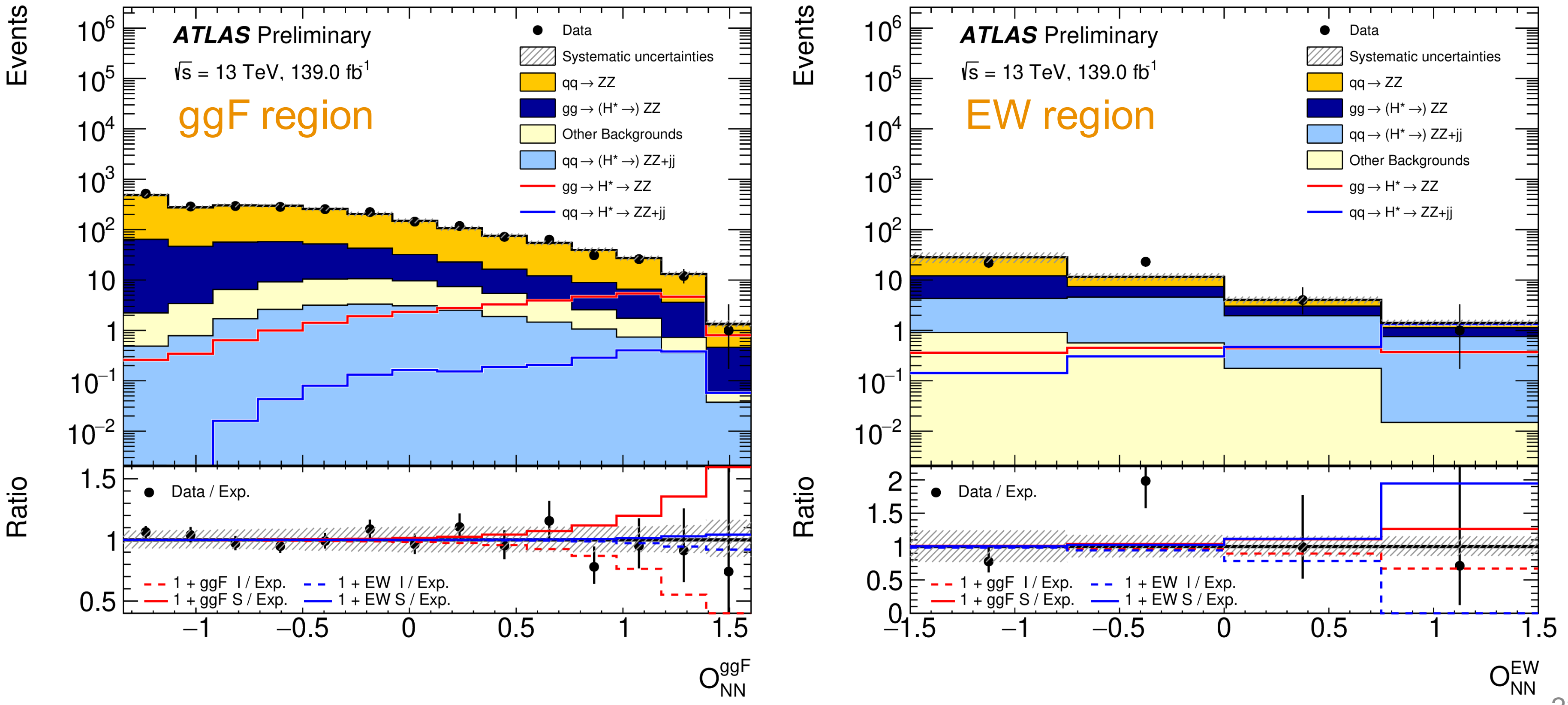

UMassAmherst

ATLAS EXPERIMENT

Observable in the $2\ell 2\nu$ channel

- The purity of off-shell Higgs production increases with m_{ZZ}
- The transverse mass is used as a proxy for the mass in the presence of neutrinos in the final state

$$(m_T^{ZZ})^2 = \left[\sqrt{m_Z^2 + (p_T^{\ell\ell})^2} + \sqrt{m_Z^2 + (E_T^{\text{miss}})^2}\right]^2 - \left|\vec{p}_T^{\,\ell\ell} + \vec{E}_T^{\text{miss}}\right|^2$$

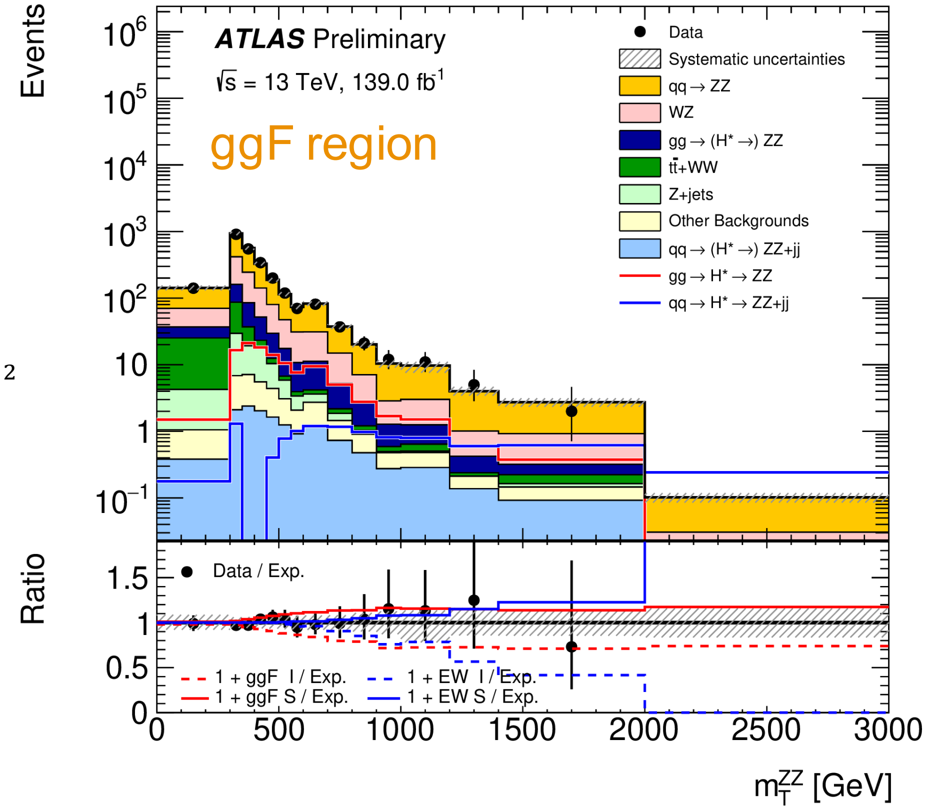

Observable in the $2\ell 2\nu$ channel

- The purity of off-shell Higgs production increases with m_{ZZ}
- The transverse mass is used as a proxy for the mass in the presence of neutrinos in the final state

$$(m_T^{ZZ})^2 = \left[\sqrt{m_Z^2 + (p_T^{\ell\ell})^2} + \sqrt{m_Z^2 + (E_T^{\text{miss}})^2}\right]^2 - \left|\vec{p}_T^{\,\ell\ell} + \vec{E}_T^{\text{miss}}\right|^2$$

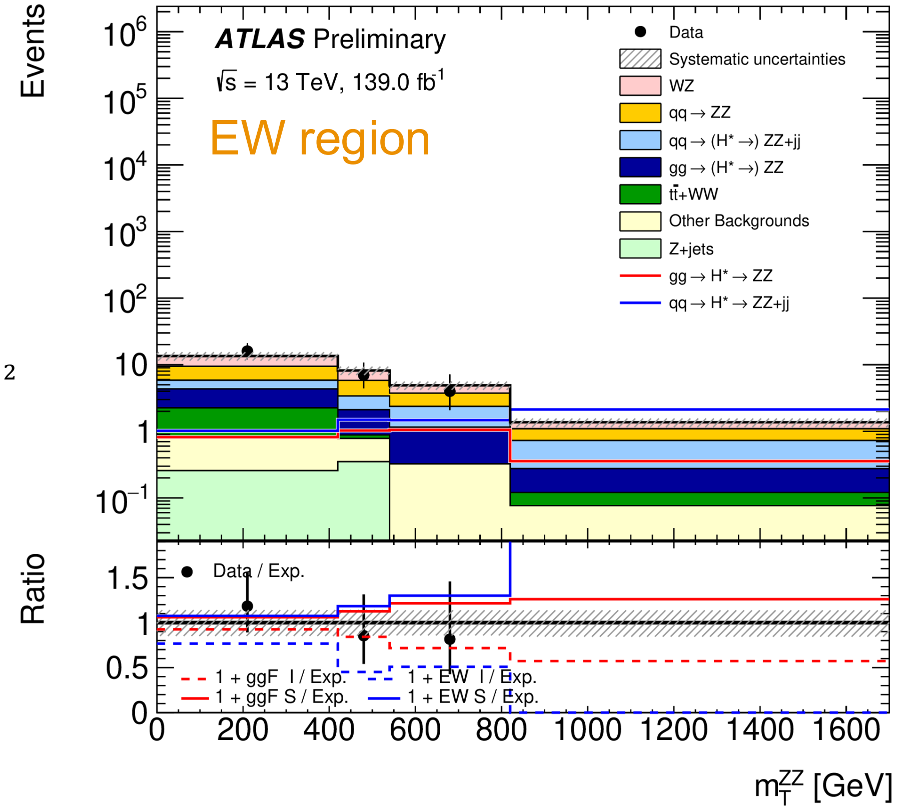

Signal and background modeling

The distribution of the observables in each channel is obtained from MC simulations

Process	MC generator	Description
ggF S, B, SBI	Sherpa v2.2.2	0+1 jets @ LO
EW SBI0, SBI1, SBI10	Madgraph5	LO
$q\bar{q}ZZ$	Sherpa v2.2.2	0+1 jets @ NLO, 2+3 jets @ LO
WZ	Sherpa v2.2.1	0+1 jets @ NLO, 2+3 jets @ LO

*subleading processes not included here

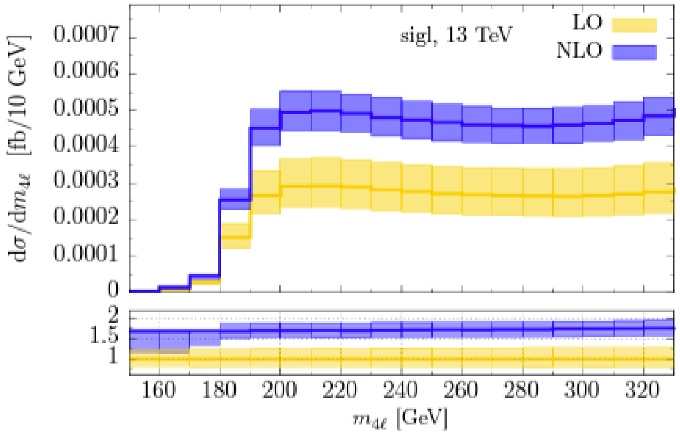

Caola et al. *JHEP* 07 (2016) 087

EW NLO corrections for $q\bar{q}ZZ$ calculated by S. Kallweit et al [11] are applied.

ggF S, B, and SBI are scaled to NLO using the calculation by F. Caola et al. from 2016 [12]. An additional factor of 1.2×1.1 is used to approximate NNLO [13] and N^{3}LO corrections.

[11] JHEP 11 (2017) 120
[12] JHEP 07 (2016) 087
[13] Eur. Phys. J. C 74 (2014) 2866

Background normalization

The normalizations of the main background sources are determined by data

- 4ℓ and $2\ell2\nu$ channels: $\mu(q\bar{q}ZZ)$
- $2\ell2\nu$ channel: $\mu(WZ)$, $\mu(Z+\text{jets})$, and non-resonant $\ell\ell$ $\mu(e\mu)$ production (mostly $t\bar{t}$ and WW)

The ratios of observed yields in jet bins

$$\frac{\mu(q\bar{q}ZZ+1\text{jet})}{\mu(q\bar{q}\text{ZZ})}, \frac{\mu(q\bar{q}ZZ+(2+)\text{jet})}{\mu(q\bar{q}\text{ZZ})}, \frac{\mu(WZ+1\text{jet})}{\mu(\text{WZ})}, \frac{\mu(WZ+(2+)\text{jet})}{\mu(\text{WZ})}$$

are also determined by data to improve the background description in the jet-binned signal regions.

Dedicated control regions are introduced to constrain each of the data-driven normalization factors.

Control regions

- Three $q\bar{q} \to ZZ$ control regions are defined in 4ℓ final state

$$180 \leq m_{4\ell} \leq 220 \text{ GeV} \qquad n_{\text{jets}} = 0, 1, \geq 2$$

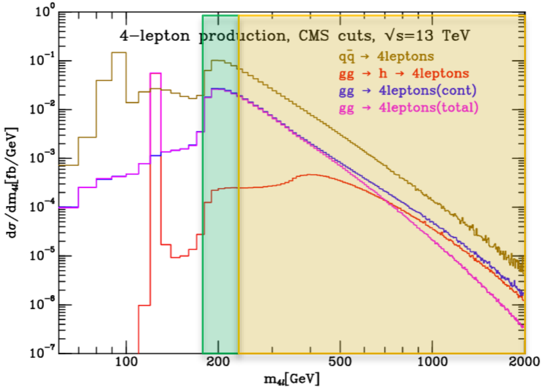

- Several control regions targeting $2\ell 2\nu$ backgrounds. Selections based on the $2\ell 2\nu$ event selection

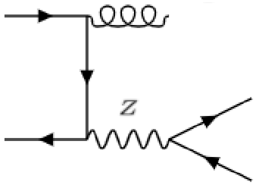

E_T^{miss} significance < 9

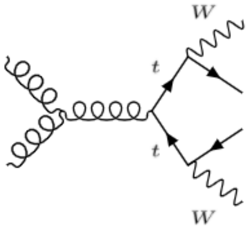

selects $e\mu$ pairs

3 regions:
$n_{\text{jets}} = 0, 1, \geq 2$

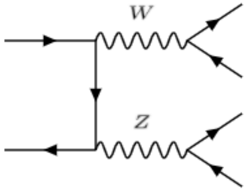

requires 3rd lepton
$m_T(3^{\text{rd}} \text{ lep}) > 60$ GeV
E_T^{miss} significance > 3

One control region per floating normalization

Modeling uncertainties

- **Scale variation** in the NLO/LO k-factor are used as missing higher-order uncertainties for ggF S, SBI, and B processes.
- Additional higher-order uncertainties estimated by varying Sherpa **resummation** and **matching** scales in both $q\bar{q} \rightarrow ZZ$ and ggF processes.
- Higher-order QCD uncertainties in $q\bar{q} \rightarrow ZZ$ estimated by **renormalization** and **factorization** scale variations.
- EW NLO uncertainties in $q\bar{q} \rightarrow ZZ$ estimated with MATRIX (by M. Grazzini et al [14]) based on the difference between the **multiplicative** and **additive schemes** QCD + EW NLO corrections.
- Uncertainties on EW SBI processes are modeled through **renormalization** and **factorization** scale variations, and Pythia shower variations.

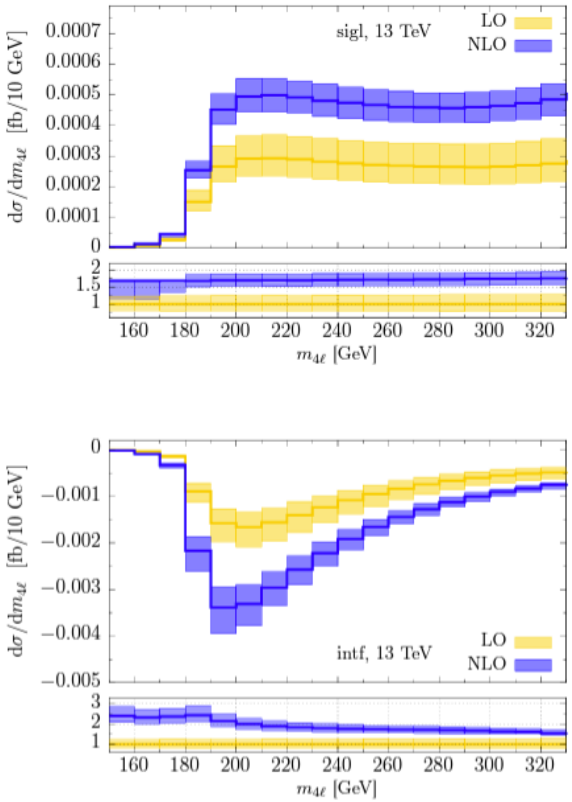

Caola et al. *JHEP* 07 (2016) 087

[14] JHEP 02 (2020) 087

Off-shell Higgs production results

UMassAmherst ATLAS EXPERIMENT

- Simultaneous fit in the six signal regions (4ℓ and $2\ell 2\nu$ channels) and eight control regions.

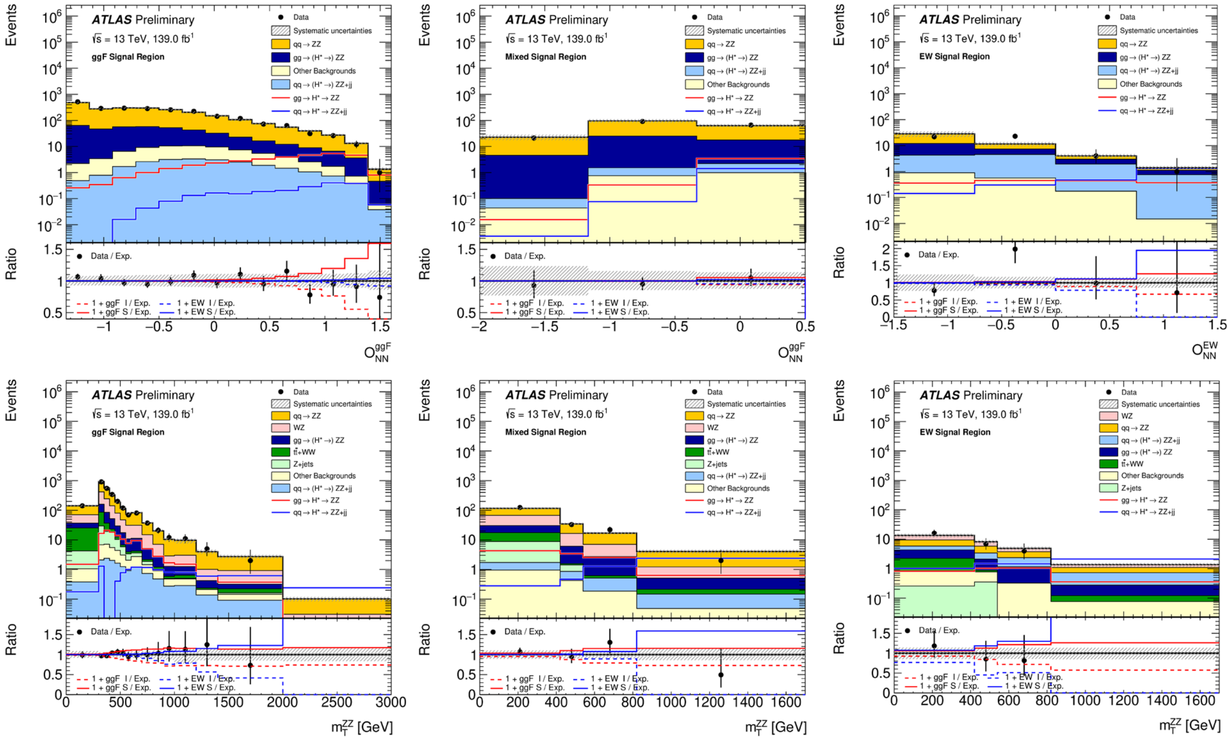

+ 8 control regions

Correlated experimental and modeling uncertainties.

Normalization factor	Fitted value
μ_{qqZZ}	1.11 ± 0.07
μ_{qqZZ}^{1j}	0.90 ± 0.10
μ_{qqZZ}^{2j}	0.88 ± 0.26
$\mu_{3\ell}$	1.06 ± 0.03
$\mu_{3\ell}^{1j}$	0.92 ± 0.10
$\mu_{3\ell}^{2j}$	0.75 ± 0.19
μ_{Zj}	0.90 ± 0.19
$\mu_{e\mu}$	1.08 ± 0.09

Off-shell Higgs production results

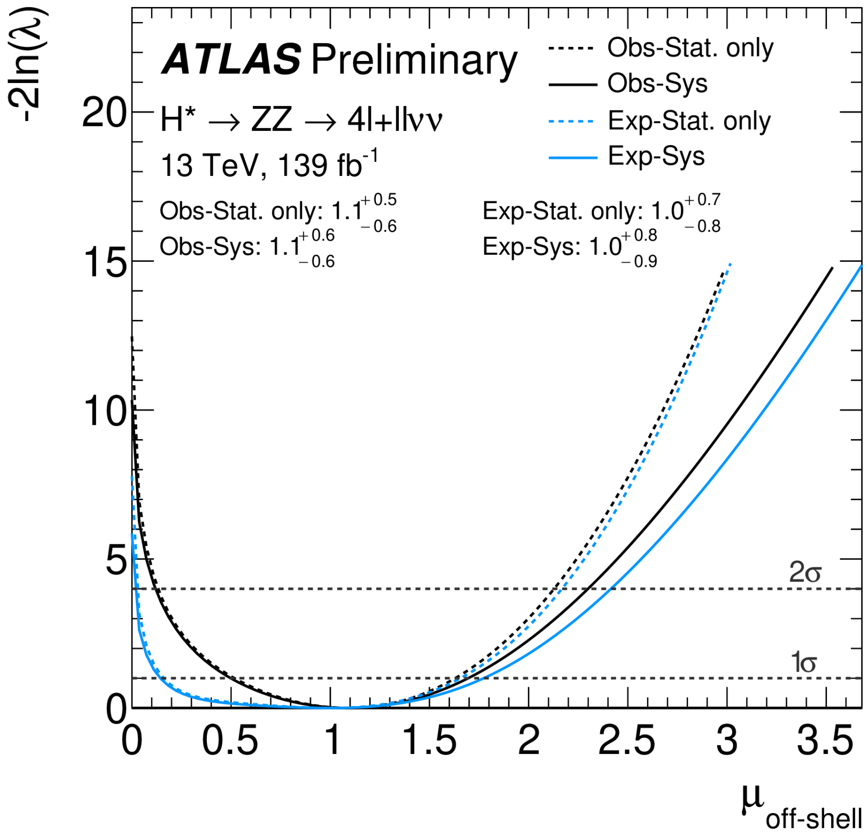

$\mu_{\text{off-shell}} = \kappa^2_{g,\text{off-shell}}\kappa^2_{V,\text{off-shell}} = \kappa^4_{V,\text{off-shell}}$

The interference creates the unorthodox shape of the test statistics $-2\ln(\lambda)$

Expected uncertainty on the signal strength does not scale with $\sqrt{L}$

Asymptotic approximation, valid within 5-10%.

Off-shell Higgs production results

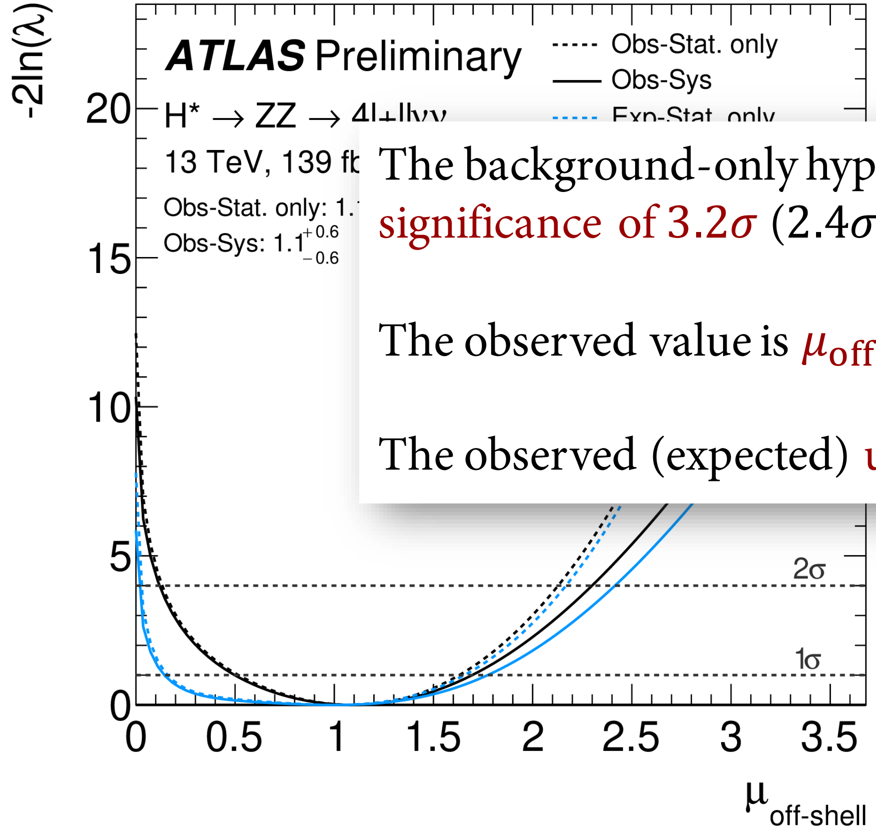

$\mu_{off-shell} = \kappa^2_{g,off-shell}\kappa^2_{V,off-shell} = \kappa^4_{V,off-shell}$

The background-only hypothesis is rejected at an observed significance of 3.2σ (2.4σ expected).

The observed value is $\mu_{off-shell} = 1.09^{+0.60}_{-0.59}$ @ 68% CL.

The observed (expected) upper limit at 95% CL. is 2.3 (2.4).

…odox shape of

…strength does not scale with $\sqrt{L}$

Off-shell Higgs production results

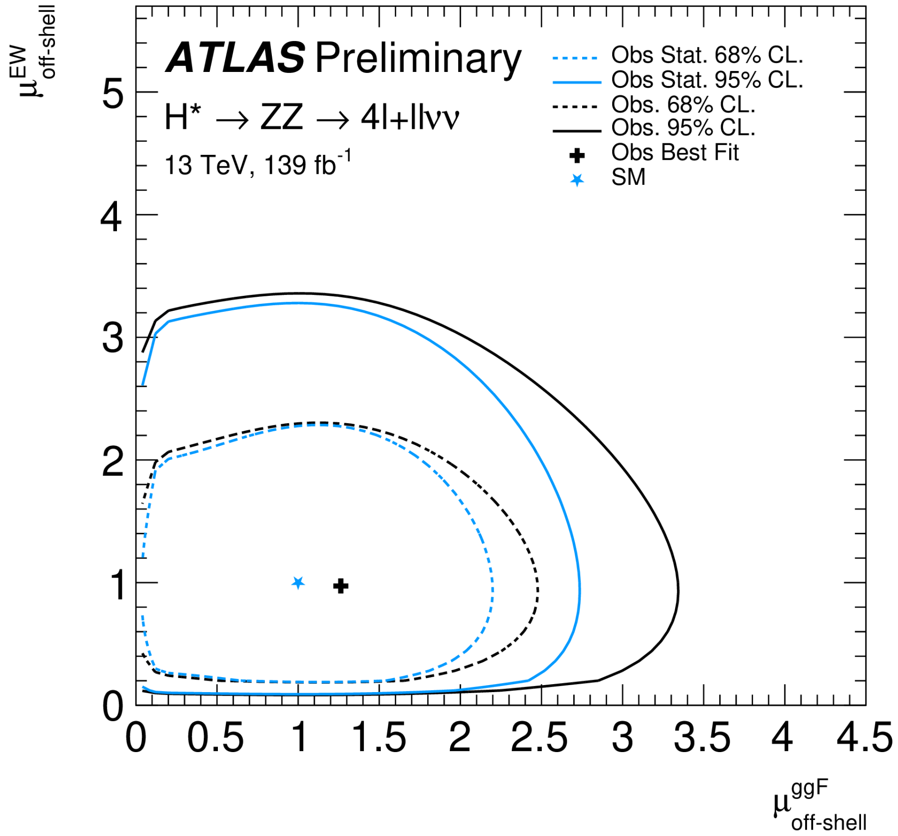

$$\mu^{\mathrm{ggF}}_{\mathrm{off-shell}} = \kappa^2_{g,\mathrm{off-shell}} \kappa^2_{V,\mathrm{off-shell}}$$
$$\mu^{\mathrm{EW}}_{\mathrm{off-shell}} = \kappa^4_{V,\mathrm{off-shell}}$$

The interference creates the unorthodox shape of the test statistics $-2\ln(\lambda)$

Expected uncertainty on the signal strength does not scale with $\sqrt{L}$

Impact of systematic uncertainties

Measurement of $\mu_{\text{off-shell}}$ is not a measurement of a yield. Interference gives rise to two different values of $\mu_{\text{off-shell}}$ for a given yield.

There are yields for which there are no solutions (not considering nuisance parameters)

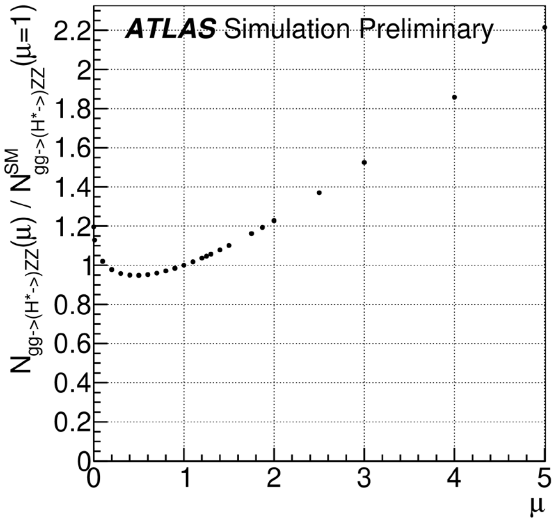

Systematic Uncertainties	$-2\ln\lambda(\mu_{\text{off-shell}}) = 4$ crossing
Parton shower uncertainty for $ggZZ$ (normalisation)	2.26
Parton shower uncertainty for $ggZZ$ (shape)	2.29
NLO EW uncertainty for $qqZZ$	2.27
NLO QCD uncertainty for $ggZZ$	2.29
Parton shower uncertainty for $qqZZ$ (shape)	2.29
Jet energy scale and resolution uncertainty	2.26
All uncertainties	2.30

Double solution for $\mu_{\text{off-shell}}$ also makes the definition of systematic uncertainty impact via finite differences $\hat{\mu}(\hat{\alpha} + \delta\alpha) - \hat{\mu}(\hat{\alpha})$ unreliable.

Impact of systematics uncertainties given instead by the change in $-2\ln(\lambda) = 4$ crossing when the given uncertainty source is removed.

Comparison with previous result

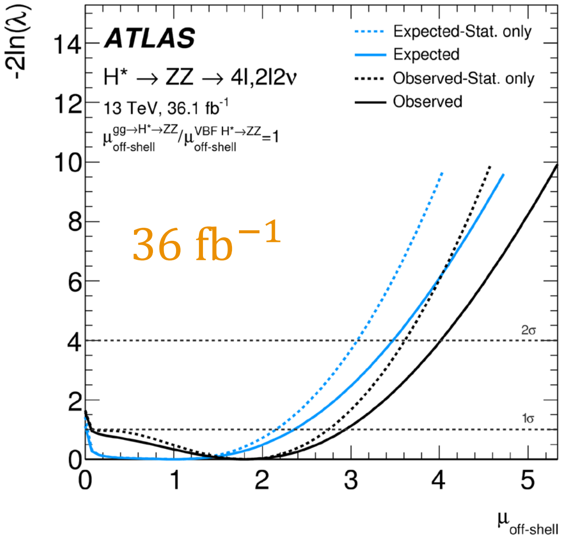

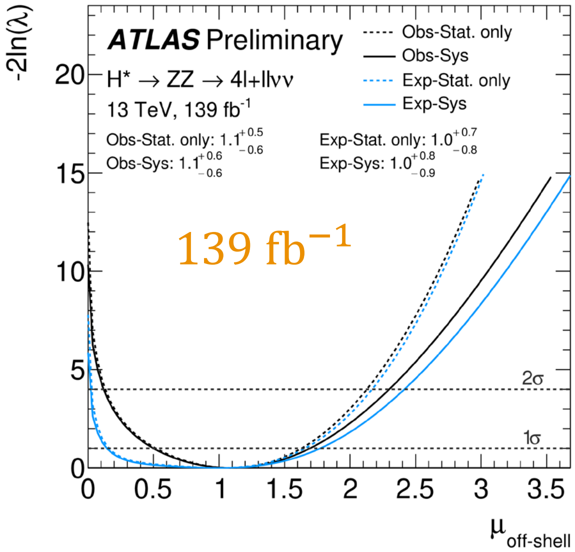

New in this preliminary result

- Increased integrated luminosity
- Optimized discriminant in the 4ℓ channel
- Improved description of modeling systematics
- Separate results for ggF and EW production

On-shell measurement results

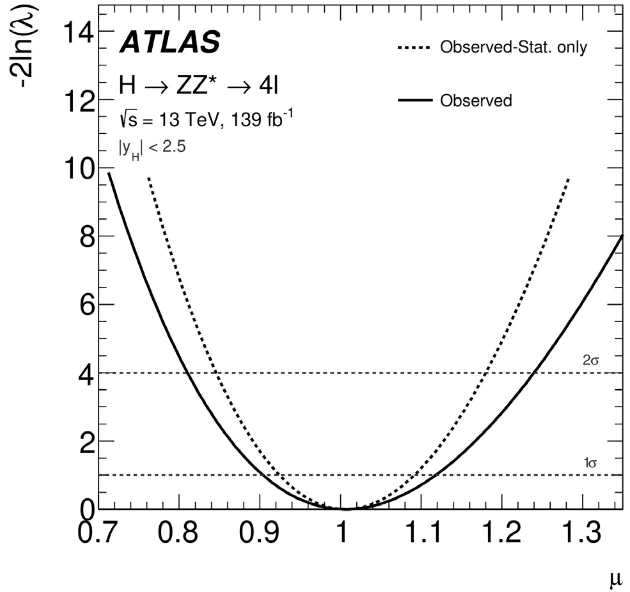

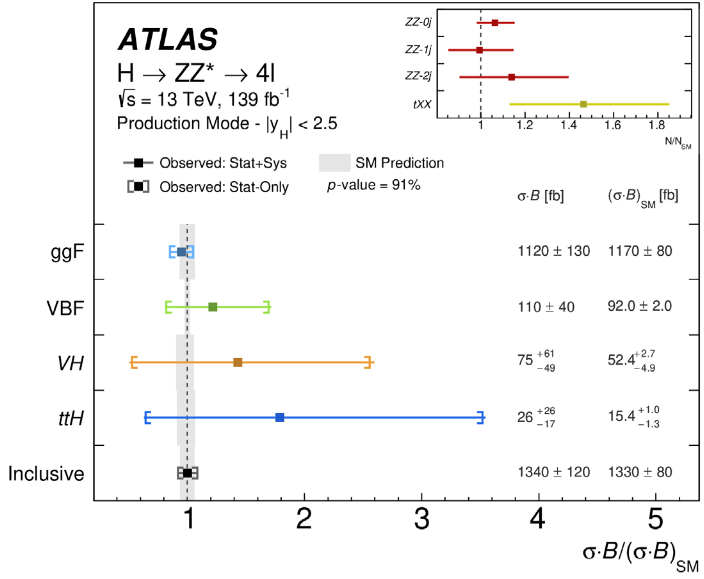

This is the on-shell only result. $\mu_{on-shell}$ is always floating when the on-shell / off-shell ratios are determined.

ATLAS Collaboration, Eur. Phys. J. C 80 (2020) 957

Off-shell/on-shell couplings

Joint off-shell ($4\ell + 2\ell 2\nu$ channel) and on-shell (4ℓ channel only) analysis

$R_{gg} = \kappa^2_{g,\text{off-shell}}/\kappa^2_{g,\text{on-shell}} = 1.37^{+0.92}_{-1.33}$

$R_{VV} = \kappa^2_{V,\text{off-shell}}/\kappa^2_{V,\text{on-shell}} = 0.9^{+0.42}_{-0.35}$

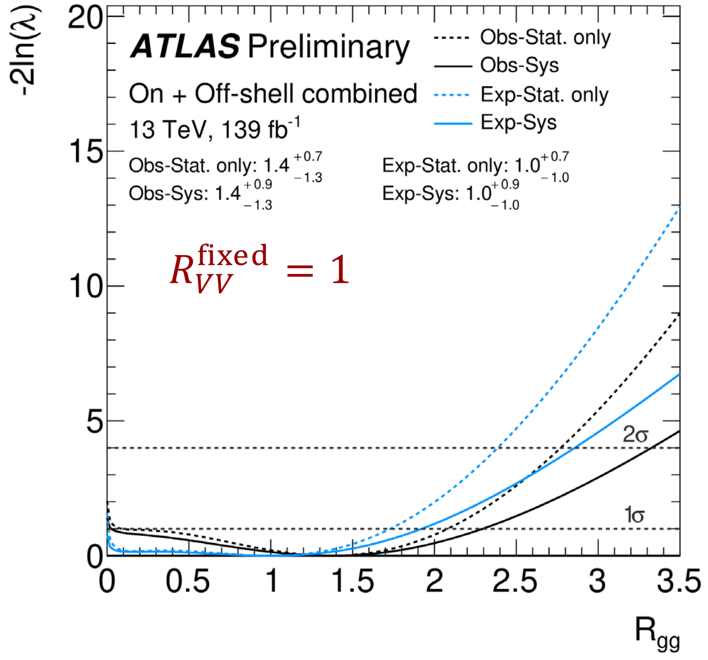

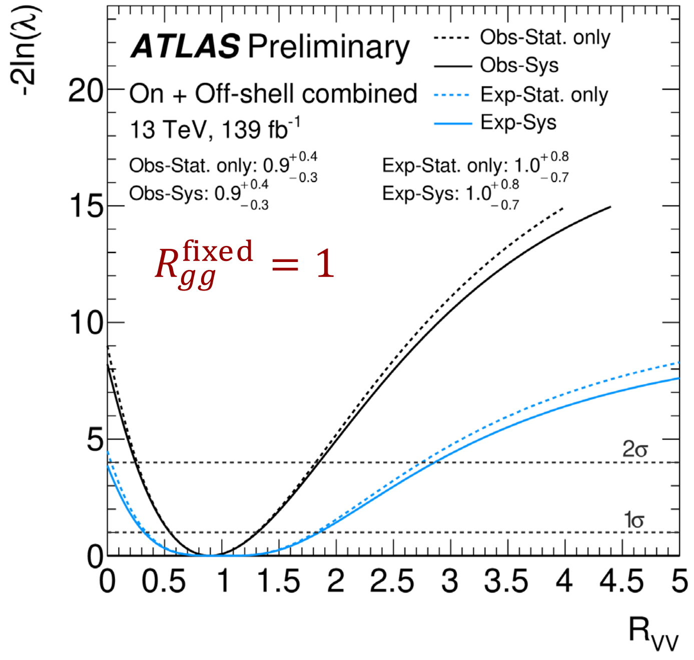

Measurement of Γ_H

- Measured ratio

$$\Gamma_H/\Gamma_H^{SM} = 1.11^{+0.63}_{-0.60}$$

- This corresponds to a measurement of the total Higgs boson width of

$$\Gamma_H = 4.6^{+2.6}_{-2.5}\text{ MeV @ 68\% CL.}$$

- Uncertainty quoted using asymptotic approximation.

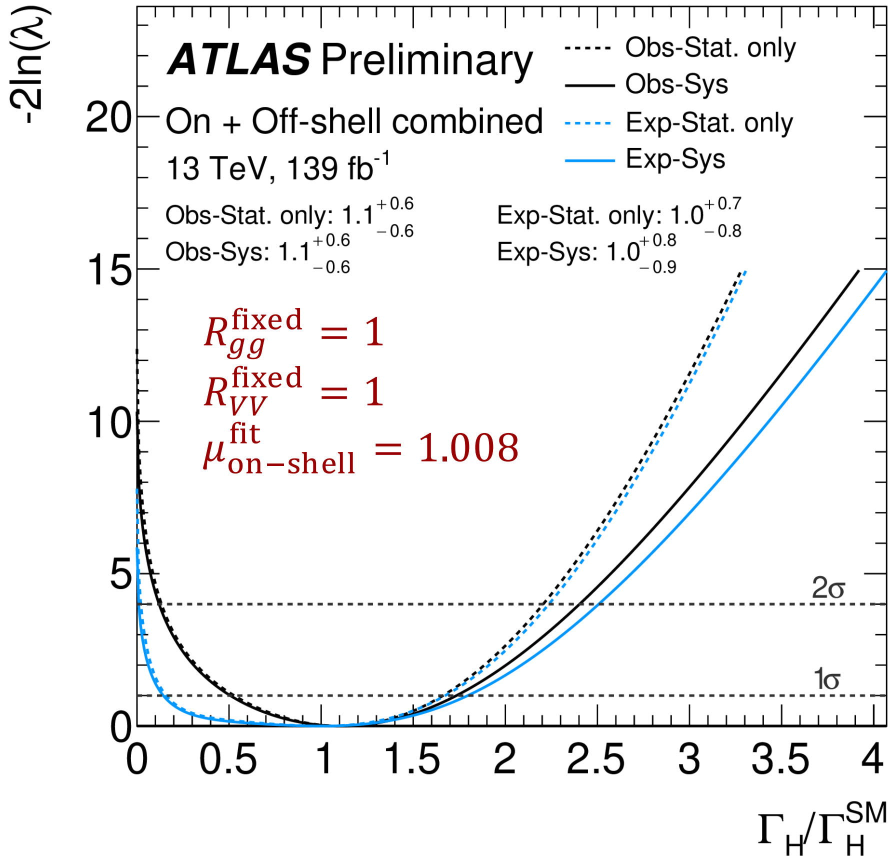

Conclusions

UMassAmherst ATLAS EXPERIMENT

- We presented a new measurement of the Higgs boson total width.
- The Higgs boson total width is probed via the measurement of the off-shell Higgs production in the $H \to ZZ \to 4\ell$ and $H \to ZZ \to 2\ell 2\nu$ channels.
- We have evidence for the off-shell production of Higgs bosons. The background-only hypothesis is rejected at an observed significance of 3.2σ (2.4σ expected).
- The measurement of the Higgs total width is

$$\Gamma_H = 4.6^{+2.6}_{-2.5}\ \text{MeV @ 68\% CL.}\ (4.1^{+3.2}_{-3.5}\ \text{MeV expected})$$

- Consistent with the recent CMS result $\Gamma_H = 3.2^{+2.4}_{-1.7}$ MeV ($4.1^{+4.0}_{-3.5}$ MeV expected) [15], which uses 140fb^{-1} 4ℓ on-shell + 78fb^{-1} 4ℓ off-shell + 138fb^{-1} $2\ell 2\nu$ off-shell.
- Several new ideas can be explored with the off-shell Higgs measurement, including searches for new heavy and light BSM states.
- This is a preliminary result. Final results and new interpretations will be provided soon.

[15] CMS Collaboration, Nat. Phys. 18 (2022) 1329